



**HAL**  
open science

## **Equine herpesvirus type 1 (EHV-1) utilizes microtubules, dynein, and ROCK1 to productively infect cells**

Arthur R. Frampton, Hiroaki Uchida, Jens von Einem, William F. Goins, Paola Grandi, Justus B. Cohen, Nikolaus Osterrieder, Joseph C. Glorioso

► **To cite this version:**

Arthur R. Frampton, Hiroaki Uchida, Jens von Einem, William F. Goins, Paola Grandi, et al.. Equine herpesvirus type 1 (EHV-1) utilizes microtubules, dynein, and ROCK1 to productively infect cells. *Veterinary Microbiology*, 2010, 141 (1-2), pp.12. 10.1016/j.vetmic.2009.07.035 . hal-00560844

**HAL Id: hal-00560844**

**<https://hal.science/hal-00560844>**

Submitted on 31 Jan 2011

**HAL** is a multi-disciplinary open access archive for the deposit and dissemination of scientific research documents, whether they are published or not. The documents may come from teaching and research institutions in France or abroad, or from public or private research centers.

L'archive ouverte pluridisciplinaire **HAL**, est destinée au dépôt et à la diffusion de documents scientifiques de niveau recherche, publiés ou non, émanant des établissements d'enseignement et de recherche français ou étrangers, des laboratoires publics ou privés.

## Accepted Manuscript

Title: Equine herpesvirus type 1 (EHV-1) utilizes microtubules, dynein, and ROCK1 to productively infect cells

Authors: Arthur R. Frampton Jr., Hiroaki Uchida, Jens von Einem, William F. Goins, Paola Grandi, Justus B. Cohen, Nikolaus Osterrieder, Joseph C. Glorioso



PII: S0378-1135(09)00357-5  
DOI: doi:10.1016/j.vetmic.2009.07.035  
Reference: VETMIC 4527

To appear in: *VETMIC*

Received date: 7-4-2009  
Revised date: 5-7-2009  
Accepted date: 31-7-2009

Please cite this article as: Frampton Jr., A.R., Uchida, H., von Einem, J., Goins, W.F., Grandi, P., Cohen, J.B., Osterrieder, N., Glorioso, J.C., Equine herpesvirus type 1 (EHV-1) utilizes microtubules, dynein, and ROCK1 to productively infect cells, *Veterinary Microbiology* (2008), doi:10.1016/j.vetmic.2009.07.035

This is a PDF file of an unedited manuscript that has been accepted for publication. As a service to our customers we are providing this early version of the manuscript. The manuscript will undergo copyediting, typesetting, and review of the resulting proof before it is published in its final form. Please note that during the production process errors may be discovered which could affect the content, and all legal disclaimers that apply to the journal pertain.

**1 Equine herpesvirus type 1 (EHV-1) utilizes microtubules, dynein, and ROCK1 to productively infect**  
**2 cells.**

**3**  
**4** Arthur R. Frampton Jr.<sup>1\*†</sup>, Hiroaki Uchida<sup>1</sup>, Jens von Einem<sup>2</sup>, William F. Goins<sup>1</sup>, Paola Grandi<sup>3</sup>, Justus B.  
**5** Cohen<sup>1</sup>, Nikolaus Osterrieder<sup>2,4</sup>, Joseph C. Glorioso<sup>1</sup>.  
**6**

**7**  
**8** <sup>1</sup>Department of Microbiology and Molecular Genetics, University of Pittsburgh, School of Medicine,  
**9** Pittsburgh, PA 15261

**10** <sup>2</sup>Department of Microbiology and Immunology, College of Veterinary Medicine, Cornell University, Ithaca,  
**11** NY 14853

**12** <sup>3</sup>Department of Neurological Surgery, University of Pittsburgh, School of Medicine, Pittsburgh, PA, 15261

**13** <sup>4</sup>Institut für Virologie, Freie Universität Berlin, 10115 Berlin Germany  
**14**  
**15**  
**16**

**17** Running Title: EHV-1 intracellular trafficking is dependent on microtubules, dynein and ROCK1  
**18**  
**19**

**20** \*To whom correspondence should be addressed

**21** †Current affiliation:

**22** Arthur R. Frampton Jr. Ph.D  
**23** Assistant Professor  
**24** University of North Carolina Wilmington  
**25** Department of Biology and Marine Biology  
**26**

**27** Phone: (910) 962-2643 Fax: (910)962-4066

**28** E-mail address: framptona@uncw.edu  
**29**  
**30**  
**31**

**32 Abstract**

**33** To initiate infection, equine herpesvirus type 1 (EHV-1) attaches to heparan sulfate on cell surfaces and then  
**34** interacts with a putative glycoprotein D receptor(s). After attachment, virus entry occurs either by direct fusion  
**35** of the virus envelope with the plasma membrane or via endocytosis followed by fusion between the virus  
**36** envelope and an endosomal membrane. Upon fusion, de-enveloped virus particles are deposited into the  
**37** cytoplasm and travel to the nucleus for viral replication. In this report, we examined the mechanism of EHV-1  
**38** intracellular trafficking and investigated the ability of EHV-1 to utilize specific cellular components to  
**39** efficiently travel to the nucleus post-entry. Using a panel of microtubule depolymerizing drugs and inhibitors of  
**40** microtubule motor proteins, we show that EHV-1 infection is dependent on both the integrity of the microtubule  
**41** network and the minus-end microtubule motor protein, dynein. In addition, we show that EHV-1 actively  
**42** induces the acetylation of tubulin, a marker of microtubule stabilization, as early as 15 minutes post-infection.  
**43** Finally, our data support a role for the cellular kinase, ROCK1, in virus trafficking to the nucleus.

**44**

**45 Keywords:** EHV-1, trafficking, microtubules, dynein, ROCK1

**46****47 1. Introduction**

**48** Equine herpesvirus 1 (EHV-1) is a major pathogen of horses. Most horses are exposed to the virus within 6  
**49** months to a year after birth and are frequently re-infected throughout their lifetime (Allen, 1986). Clinical signs  
**50** that appear early after infection include fever, inappetence, malaise, coughing, and mucopurulent discharge  
**51** (O'Callaghan et al., 1983). As the infection progresses, horses may exhibit signs of serious neurological illness  
**52** including ataxia, disorientation, and partial to full paralysis. In addition to the neurological sequelae, EHV-1  
**53** also causes abortigenic disease in pregnant mares.

**54** At the cellular level, EHV-1 must engage host cellular proteins and induce specific signaling pathways very  
**55** early in infection in order to successfully infect cells. EHV-1 initially binds to target cells via an interaction  
**56** between viral glycoproteins B and C and glycosaminoglycans on the plasma membrane (Sugahara et al., 1997,  
**57** Osterrieder, 1999). After attachment, a putative entry receptor is recognized (Frampton et al., 2005) by

58 glycoprotein D (Csellner et al., 2000). The next step in the EHV-1 entry pathway varies depending upon the cell  
59 type (Frampton et al., 2007). EHV-1 fuses with the plasma membrane and deposits de-enveloped particles into  
60 the cytoplasm of equine dermal (ED) and rabbit kidney (RK-13) cells. On the contrary, fully enveloped particles  
61 are endocytosed in CHO-K1 cells and naked capsids are then released into the cytosol after the virus fuses with  
62 the endosomal membrane. Regardless of the initial mode of entry, we recently showed that the cellular kinase  
63 Rho associated coiled-coil kinase 1 (ROCK1) must be induced for the virus to complete the infection process  
64 (Frampton et al., 2007).

65 Once inside the cells, EHV-1 must traverse the intricate meshwork of the intracellular cytoskeleton in order  
66 to reach the nucleus and deposit the viral genome. The mechanisms employed by EHV-1 to traffic to the  
67 nucleus have yet to be defined, but certain clues are provided by studies with other viruses that utilize  
68 microtubules and their associated machinery for intracellular trafficking. Microtubules are composed of  $\alpha$  and  $\beta$   
69 dimers of tubulin and contain a structural polarity with a positive end that is oriented toward the periphery of  
70 the cell and a negative end that is anchored at the microtubule organizing center (MTOC) adjacent to the  
71 nucleus (Nogales, 2000). To reach the nucleus, many viruses attach themselves to, and are directionally  
72 propelled by dynein, a minus-end directed microtubule motor, towards the MTOC (Kelkar et al., 2004, Alonso  
73 et al., 2001, Suikkanen et al., 2003, Petit et al., 2003, Ye et al., 2000, Douglas et al., 2004, Jacob et al., 2000,  
74 Raux et al., 2000, Florin et al., 2006). Sodeik et al. initially showed that the alphaherpesvirus herpes simplex  
75 virus type 1 (HSV-1) uses microtubules to traffic to the nucleus. Their data revealed that nuclear transport of  
76 HSV-1 was significantly inhibited in the presence of the microtubule-depolymerizing drugs, nocodazole,  
77 vinblastine, or colchicine (Sodeik et al., 1997). The movement of HSV-1 capsids along microtubules was also  
78 shown to require dynein as expression of the dynein inhibitor, dynamitin (Dohner et al., 2002), and specific  
79 inhibitors of dynein ATPase (Lee et al., 2006, Kobayashi et al., 1978, Kristensson et al., 1986, Penningroth et  
80 al., 1982) decreased HSV-1 transport to the nucleus. The movement of virus particles was also shown to be  
81 independent of microtubule turnover or treadmilling (microtubule polymerization/depolymerization) as the  
82 microtubule-stabilizing drug paclitaxel had no effect on nucleocapsid transport (Sodeik et al., 1997).

83 In addition to utilizing microtubules for transport, viruses also generate an intracellular environment that is  
84 conducive for nuclear transport by triggering various signaling pathways. One common theme is the induction  
85 of signaling pathways that lead to the reorganization of cytoskeletal components. Many viruses, including HSV-  
86 1, stimulate members of the Ras GTPase superfamily and this induction can lead to a wide array of  
87 morphological changes of infected cells, including, but not limited to, stabilization of microtubules (Naranatt et  
88 al., 2005), formation of focal adhesions (Cheshenko et al., 2005) and endocytosis or phagocytosis (Clement et  
89 al., 2006).

90 In this study, we show that EHV-1 causes the stabilization of microtubules via the acetylation of tubulin and  
91 utilizes the minus-end directed microtubule motor dynein to traffic to the nucleus along stabilized microtubules.  
92 In addition, we show that nuclear accumulation of capsids is decreased in the presence of the ROCK1 inhibitor,  
93 Y-27632.

## 94 2. Materials and methods

### 95 2.1. Cells, viruses, and plasmids

96  
97  
98 RK-13 cells were grown in Dulbecco's modified Eagle medium (DMEM) supplemented with 10% fetal  
99 bovine serum (FBS) (Invitrogen, Carlsbad, CA). Chinese hamster ovary (CHO-K1) cells were kindly provided  
100 by Dr. Patricia Spear (Northwestern University, Chicago, IL) and grown in F12-K media (Invitrogen)  
101 supplemented with 10% FBS. Equine dermal cells (ED), a gift from Dr. Ron Montelaro (University of  
102 Pittsburgh, Pittsburgh, PA), were maintained in minimal essential medium (MEM) supplemented with 10%  
103 FBS. All cells were maintained at 37°C in 5% CO<sub>2</sub>.

104 The EHV-1 recombinant virus L11ΔgIΔgE contains a *lacZ* reporter cassette in place of gI and gE (Frampton  
105 et al., 2002). The EHV-1 recombinant virus L11VP26mRed was described previously (J. von Einem et al., 24<sup>th</sup>  
106 annual ASV meeting 2005). This recombinant virus contains an mRFP1 fluorescent protein fused to the EHV-1  
107 VP26 small capsid protein.

### 108 2.2. Drug inhibition assays

110 For entry assays,  $2.5 \times 10^4$  ED or CHO-K1 cells were seeded in a 96-well plate. The next day, cells were  
111 incubated with increasing amounts of the microtubule depolymerizing drugs, nocodazole, vinblastine,  
112 colchicine, the microtubule stabilizing drug, paclitaxel (PTX), the dynein inhibitor, EHNA (erythro-9-(2-  
113 hydroxy-3-nonyl) adenine, or the kinesin inhibitor AMP-PNP (adenosine 5'-( $\beta$ ,  $\gamma$ -imido) triphosphate  
114 tetralithium salt) (Sigma, St. Louis, MO) at 37°C for 30 min. Cells were infected with EHV-1 (L11 $\Delta$ gI $\Delta$ gE) at  
115 an MOI of 5 and incubated for 5.5 h in the presence of the drugs at 37°C. Cells were washed once with PBS and  
116 then ONPG was added to the cells and the absorbance read at 405nm. Triplicate samples were measured for  
117 each concentration of drug. A 1mM stock of paclitaxel was prepared in distilled H<sub>2</sub>O. One-hundred mM stock  
118 solutions of EHNA and nocodazole were prepared in DMSO. A 100 mM stock solution of AMP-PNP was  
119 prepared in H<sub>2</sub>O. 10 mM stocks of the ROCK1 inhibitor, Y-27632 (EMD Biosciences, La Jolla, CA) were made  
120 in H<sub>2</sub>O. 10mM stocks of vinblastine, and colchicine were also made in H<sub>2</sub>O. Cell viability was measured in  
121 triplicate using the CellTiter 96 aqueous non-radioactive cell proliferation assay (Promega, Madison, WI)  
122 following the manufacturer's protocol.

### 123 2.3. Western Blot Analyses

124  
125  
126 Confluent ED cells in a 12-well plate were serum starved for 1 h and cells were then mock-treated or treated  
127 with paclitaxel (10  $\mu$ M) or Y-27632 (100  $\mu$ M). Cells treated with paclitaxel were washed with MEM at 15, 30,  
128 and 60 min and cell lysates were harvested with PARP lysis buffer (6 M urea, 2% SDS, 10% glycerol, 62.5 mM  
129 Tris-HCl, pH 6.8, and 5%  $\beta$ -mercaptoethanol). Mock-treated cells or cells treated with Y-27632 were infected  
130 with EHV-1 (L11VP26mRed) at an MOI of 10 in the presence or absence of Y-27632. At 15, 30, and 60 min  
131 post-infection, cells were washed once with MEM and lysates were harvested with PARP lysis buffer. Samples  
132 were run on a 10% SDS-PAGE gel and transferred to an immobilon-P membrane (Millipore, Billerica, MA).  
133 The membranes were blocked for 1 h in 10% non-fat dry milk (NFDM) at room temperature (RT) before  
134 monoclonal anti-acetylated tubulin antibody 6-11B-1 (Sigma) was added at a concentration of 1:2000 in TBST  
135 with 5% NFDM for 16 h at 4°C. The membranes were washed 3x for 10 min/wash and then anti-mouse-HRP

136 antibody SC-2031 (Santa Cruz Biotechnology, Santa Cruz, CA) was added at a concentration of 1:3,000 in  
137 TBST with 5% NFDM for 1 h at RT. Membranes were washed 3x for 10 min/wash then ECL detection reagent  
138 (Amersham Biosciences, Buckinghamshire, England) was added and the membranes exposed to film. After  
139 stripping the membrane with stripping buffer (10% SDS, 0.5M Tris pH 6.8, 0.5%  $\beta$ -mercaptoethanol) for 30  
140 min at 50°C, the membranes were washed 2x for 10 min/wash with TBST and then blocked for 1 h with 10%  
141 NFDM. Total tubulin was detected by adding monoclonal anti- $\alpha$ -tubulin antibody B-5-1-2 (Sigma) at 1:2,000  
142 for 16 h at 4°C with the secondary antibody and detection steps as described earlier.

143

#### 144 *2.4. Infectious virus recovery assay*

145  $4 \times 10^5$  cells in 24-well plates were incubated with 100  $\mu$ M of Y-27632 in DMEM or DMEM alone for 30  
146 min at 37°C. Plates were placed on ice for 5 min and then EHV-1 (MOI = 10) in DMEM or DMEM containing  
147 100  $\mu$ M Y-27632 was incubated on the cells at 4°C for 3 h. Cells were washed once with cold DMEM and then  
148 warm media (37°C) was added to the cells. At each time-point, cells were washed with glycine (pH 3.0) for 30  
149 s, washed once with DMEM, and harvested. Virus samples were freeze-thawed once then sonicated 3x for 15 s.  
150 Virus harvested from each time-point was titered on RK13 cells. Triplicate samples were measured for each  
151 time-point.

152

#### 153 *2.5. Confocal microscopy of EHV-1 infected cells*

154 CHO-K1 cells were seeded to confluency in collagen-coated 35 mm dishes (MatTek Corporation, Ashland,  
155 MA). Cells were mock-treated or treated with 100  $\mu$ M Y-27632 or 10  $\mu$ M paclitaxel for 30 min at 37°C. Cells  
156 were chilled on ice for 10 min and then L11VP26mRed was added to the cells at an MOI of 10. Virus was  
157 incubated on the cells at 4°C for 2 h in the presence or absence of drug. After 2 h, cells for the 0 time-point were  
158 fixed with 4% paraformaldehyde (PFA) at 4°C. Media pre-warmed to 37°C, with or without drug, was added to  
159 the remaining cells and then the cells were fixed with 4% PFA at 15, 30, 60, and 120 min post temperature shift.  
160 After 30 min of fixation with 4% PFA, cells were rehydrated with PBS for 15 min at 4°C. Cells were washed

once more with PBS for 15 min and then cells were examined using an inverted Olympus Fluo-View 1000 confocal microscope (Olympus America Inc., Center Valley, PA). Prior to imaging, cells were stained with Hoechst dye (1  $\mu\text{g}/\text{mL}$ ) and wheat germ agglutinin (5  $\mu\text{g}/\text{mL}$ ) to label the nucleus and plasma membrane, respectively. All images were captured at a 60x magnification.

### 3. Results

#### 3.1. EHV-1 utilizes microtubules for infection

To determine if EHV-1 requires microtubules for infection, a virus entry assay was performed in the presence or absence of microtubule depolymerizing agents. Equine dermal (ED) cells were untreated or treated with increasing concentrations of nocodazole, vinblastine, or colchicine for 30 min prior to infection and the drugs were kept on the cells throughout the experiment. Cells were infected with L11 $\Delta\text{gI}\Delta\text{gE}$ , an EHV-1 recombinant virus containing a *lacZ* reporter gene, at an MOI of 5 for 5.5 hours. EHV-1 infection, as measured by  $\beta$ -galactosidase expression, was significantly inhibited in a dose-dependent manner by all of the drugs. Nocodazole inhibited infection by 80% at the highest concentration tested (Figure 1A) and vinblastine (Figure 1B) and colchicine (Figure 1C) inhibited infection by 82% and 56%, respectively. This inhibition of infection was not the result of drug-associated cell toxicity as cell viability was similar for all of the concentrations used. In addition to inhibiting infection on ED cells, these drugs also inhibited infection on CHO-K1 cells (data not shown). These results indicate that an intact microtubule network is required regardless of the mode of EHV-1 entry.

To address the importance of microtubule dynamics or treadmilling (polymerization/depolymerization of microtubules) in virus transport, microtubules were first stabilized with paclitaxel or left untreated before and during infection with EHV-1. Virus entry was assessed by measuring  $\beta$ -galactosidase activity 5.5 h post-infection. In both ED (Fig 2A) and CHO-K1 (Fig 2B) cells, stabilization of microtubules prior to the addition of EHV-1 had no effect on infection as measured by viral reporter gene expression. To assure that paclitaxel treatment of ED cells induced microtubule stabilization, we examined the acetylation of tubulin, which has been

188 shown to be a reliable indicator of stable or fixed microtubules (Piperno et al., 1987). Western blotting was  
189 performed to detect acetylated tubulin at 15, 30, and 60 minutes post-treatment with 10  $\mu$ M paclitaxel. As  
190 shown in Figure 3, paclitaxel treatment resulted in the hyperacetylation of tubulin as early as 15 minutes post-  
191 treatment and the level of acetylation steadily increased the longer the cells were treated with the drug.

192 The ability of EHV-1 to travel to the nucleus after microtubule stabilization was assessed by infecting CHO-  
193 K1 cells with the fluorescently tagged-EHV-1 recombinant L11VP26mRed in the presence or absence of  
194 paclitaxel. This recombinant virus contains a red fluorescent protein fused to the VP26 capsid protein and thus  
195 the subcellular localization of this virus can be detected throughout a time course of infection by confocal  
196 microscopy. CHO-K1 cells were untreated or treated with 10  $\mu$ M of paclitaxel for 30 minutes and then virus  
197 was added and allowed to attach to the cells at 4°C for 2 hours to synchronize the entry process. After  
198 attachment, medium warmed to 37°C, with or without addition of the drug, was added to the cells to allow  
199 infection to ensue. At 0 and 60 minutes post-temperature shift, cells were stained with Hoechst dye and wheat  
200 germ agglutinin to label the nucleus (blue) and plasma membrane (green), respectively. As shown in Figure 4,  
201 attached virus (red) was detected on the surface of mock-treated and paclitaxel-treated cells at the 0 time-point.  
202 At the 60-minute time-point, a similar number of capsids were observed at the nucleus in both mock-treated and  
203 paclitaxel-treated cells. The ability of virus to reach the nucleus after paclitaxel stabilization of microtubules in  
204 a manner similar to that observed in mock-treated cells suggests that EHV-1 is efficiently transported along  
205 stable microtubules and that there is not a requirement for a continuous process of microtubule  
206 polymerization/depolymerization (treadmilling) for successful delivery of EHV-1 to the nucleus.

### 207 208 *3.2. EHV-1 infection induces the acetylation of tubulin*

209 The ability of EHV-1 to traffic along stable microtubules led us to ask whether EHV-1 actively induces the  
210 stabilization of microtubules. To test this possibility, we compared the amount of acetylated tubulin between  
211 mock and EHV-1 infected cells by western blot assay. Other viruses, including HSV-1 (Elliott and O'Hare,  
212 1998), KSHV (Naranatt et al., 2005, Raghu et al., 2007) and African Swine Fever Virus (Jouvenet et al., 2004)

213 have been shown to induce the acetylation of tubulin upon infection and in some cases this event has been  
214 linked to the activity of Rho-signaling proteins (Naranatt et al., 2005, Raghu et al., 2007). Since ROCK1 is a  
215 proximal effector of Rho signaling, we also tested whether the inhibition of ROCK1 would have any effect on  
216 the ability of EHV-1 to induce the acetylation of tubulin. ED cells were untreated or treated with the ROCK1  
217 inhibitor Y-27632 for 30 min and then either mock-infected or infected with EHV-1 at an MOI of 10 for 15, 30,  
218 and 60 minutes. As shown in Figure 5, EHV-1 infection resulted in a significant induction of acetylated tubulin  
219 as early as 15 minutes post-infection and the amount of acetylated tubulin increased over time. The ROCK1  
220 inhibitor had no effect on the ability of EHV-1 to cause the acetylation of tubulin. These results indicate that  
221 EHV-1 actively induces the acetylation of microtubules and that this process is not dependent upon the  
222 activation of ROCK1.

### 223 224 *3.3. The microtubule motor, dynein, is essential for EHV-1 infection*

225 Dynein is a minus-end directed motor that transports intracellular cargo along microtubules and many  
226 intracellular pathogens, including HSV (Sodeik et al., 1997), have been shown to utilize dynein for transport to  
227 the nucleus. To determine if EHV-1 needs dynein for efficient transport to the nucleus and thus infection, we  
228 utilized the dynein inhibitor, EHNA, which blocks the ability of dynein to hydrolyze ATP (Ravikumar et al.,  
229 2005, Penningroth et al., 1982, Bouchard et al., 1981, Dhani et al., 2003, Cheung et al., 2004). ED cells were  
230 infected with L11ΔgIΔgE in the presence or absence of EHNA and β-galactosidase expression was measured as  
231 an indicator of virus infection (Fig. 6A). As a control, cells were treated with AMP-PNP, which inhibits the  
232 plus-end directed motor, kinesin. Infection was significantly reduced in cells treated with EHNA, but not in  
233 cells treated with AMP-PNP. At the highest concentration of EHNA tested (1 mM), infection was inhibited by  
234 68%. Neither drug was toxic to the cells at the concentrations used as measured by an MTS cell viability assay.  
235 The inhibition of EHV-1 infection by EHNA indicates that EHV-1 utilizes dynein for movement to the nucleus  
236 post-entry.

237 Since the initial entry process of EHV-1 in CHO-K1 cells is different from entry into ED cells, we asked  
238 whether dynein was also employed for intracellular movement of EHV-1 in CHO-K1 cells. Entry of EHV-1

239 into CHO-K1 cells was also inhibited by EHNA in a dose-dependent manner (Fig 6B). These data suggest that,  
240 while the initial entry of EHV-1 into different cell types is dissimilar, the virus uses the same molecular  
241 machinery for transport post-entry.

#### 242 243 *3.4. Inhibition of ROCK1 deregulates the intracellular processing of EHV-1*

244 In a previous study, we showed that the activation of ROCK1 is critical for productive EHV-1 infection  
245 (Frampton et al., 2007). One possible step that ROCK1 might be required for in the EHV-1 life cycle is at the  
246 initial stage of virus uptake into cells. To test this possibility, we performed an infectious virus recovery assay  
247 on CHO-K1 cells in the presence or absence of the ROCK1 inhibitor, Y-27632. This assay allows for the  
248 recovery of fully enveloped virus particles from endosomal vesicles at different time points post-infection.  
249 CHO-K1 cells were untreated or treated with Y-27632 for 30 min at 37°C (Fig. 7). Cells were then chilled to  
250 4°C and EHV-1 was added with or without drug and allowed to attach to cells for 3 hours at 4°C. After virus  
251 attachment, the temperature was raised to 37°C and virus was incubated on cells for up to 3 hours in the  
252 presence or absence of Y-27632. At the indicated times post-temperature shift, extracellular virus was  
253 inactivated by washing the cells with an acidic buffer, and intracellular virus was harvested and titered as  
254 described in materials and methods. No difference was observed in the amount of infectious virus recovered at  
255 15 minutes, indicating that ROCK1 did not exert an effect on initial EHV-1 uptake into cells. However, there  
256 was a significant spike in the amount of virus recovered at the 30-minute time-point in the presence of Y-27632.  
257 After the 30-minute time point the amount of virus recovered from untreated and Y-27632 cells was virtually  
258 the same. The increased recovery of virus at 30 minutes in the presence of the ROCK1 inhibitor suggests that  
259 ROCK1 mediates its effect at a time post virus entry.

#### 260 261 *3.5. Decreased nuclear localization of EHV-1 in the presence of the ROCK1 inhibitor, Y-27632*

262 To examine if ROCK1 inhibition disrupts EHV-1 trafficking, CHO-K1 cells were infected with the  
263 fluorescent EHV-1 recombinant virus L11VP26mRed in the presence or absence of the ROCK1 inhibitor, Y-

27632 (Fig. 8). Cells were untreated (Fig. 8A) or treated with Y-27632 (Fig. 8B) for 30 minutes at 37°C and then virus was added and allowed to attach to cells for 2 hours at 4°C. After the attachment period, cells were warmed to 37°C to allow for virus entry. Infected cells were fixed and imaged at 0 to 120 minutes post-temperature shift using a confocal microscope. At the 0 time-point, virus particles were attached to the plasma membrane (yellow circles) and no particles were observed inside either the untreated or Y-27632-treated cells. At 15 minutes post-infection, internal and external virus particles were observed in both groups. Interestingly, as shown in Figure 8A about one-third of the virus particles were localized to the nucleus in the mock-treated cells (white circles) at 15 minutes post-infection, but only two virus particles were observed at the nucleus in the Y-27632-treated cells (Fig. 8B). Over the course of infection, more virus particles accumulated at the nucleus in the untreated cells (Fig. 8A) compared to the cells treated with Y-27632 (Fig. 8B) and the majority of particles in the Y-27632-treated cells remained associated with the plasma membrane. These data show that treatment of cells with Y-27632 significantly inhibits the movement of EHV-1 to the nucleus and indicate that ROCK1 is critical for the intracellular trafficking of EHV-1.

#### 4. Discussion

Many viruses exploit the cellular machinery to travel intracellularly. One common theme that has emerged as an integral part of the lifecycle of viruses is the co-opting of cellular motors, which are normally used to traffic various cargoes throughout the cell. Upon entry into cells, many viruses bind to molecular motors that are tethered to microtubules [for review see (Dohner et al., 2005)]. Microtubules are dynamic structures that act as cellular tracks, which viruses utilize to move directionally toward the nucleus of the cell where replication ensues. After replication and assembly, viruses utilize another set of cellular motors for egress. Without the use of these cellular motors for transport, viruses would never be able to find their way through the dense and intricate cytoskeletal structures and would thus fail to replicate and release progeny virus.

In this study, we show that EHV-1 utilizes the microtubule network and the minus-end directed motor protein dynein to productively infect cells. Disruption of the microtubular network with the microtubule

289 depolymerizing agents nocodazole, vinblastine, and colchicine inhibited the ability of EHV-1 to productively  
290 infect cells and deliver its payload to the nucleus. In addition, the introduction of dynein, but not kinesin  
291 inhibitors, also reduced infection. Interestingly, microtubules and dynein were required for virus trafficking in  
292 cells that were infected via an endocytic route or by direct fusion of virus at the plasma membrane. These data  
293 suggest at least two possible models for intracellular trafficking of EHV-1 particles that we have designated as  
294 the direct and the indirect trafficking model. In the direct model, nucleocapsids that are still surrounded by some  
295 tegument proteins would bind to dynein via a viral capsid or tegument protein and this event would therefore  
296 occur only after completion of the fusion event between the viral envelope and either the plasma or endosomal  
297 membrane. In the indirect model, EHV-1 would be transported within an endosome and an endosomal protein  
298 or complex would interact with dynein. Virus would then fuse and be released from the endosome once it is in  
299 close proximity to the nucleus. The ability of EHV-1 to enter some cells by direct fusion at the cell membrane  
300 implies that a direct interaction between a viral protein and a dynein component most likely has to occur for the  
301 virus to traffic to the nucleus. However, since EHV-1 enters other cell types via an endocytic mechanism, it is  
302 possible that the indirect model of trafficking applies in these cells and thus the mechanism of intracellular  
303 movement of virus toward the nucleus may be cell-type dependent. Studies are currently underway using  
304 L11VP26mRed in conjunction with dynein and endosomal marker antibodies to further explore these models.

305 An intriguing finding from this study is the importance of the Rho kinase, ROCK1, for intracellular  
306 trafficking of EHV-1 particles. Previously, we showed that inhibition of this kinase significantly reduced EHV-  
307 1 infection (Frampton et al., 2007), but we did not address the mechanism. In the current study, we showed that  
308 treatment with a ROCK1 inhibitor significantly decreased the number of capsids that accumulated at the  
309 nucleus suggesting a role for ROCK1 in the intracellular trafficking of EHV-1.

310 While this is the first report to connect ROCK1 activation with virus trafficking, previous studies have  
311 shown that other molecules involved in the ROCK1 signaling pathway also contribute to virus movement  
312 within cells. Naranatt and colleagues reported that inactivation of the RhoA GTPase, which acts directly  
313 upstream of ROCK1, blocks the delivery of KSHV to the nucleus (Naranatt et al., 2005). In addition, their data  
314 support a model in which virus binding to cells activates RhoA, which in turn leads to microtubule stabilization

315 via acetylation and an increased ability of the virus to traffic towards the nucleus (Raghu et al., 2007). This  
316 microtubule stabilization was further shown to occur after induction of Dia-2 (Naranatt et al., 2005) a member  
317 of the diaphanous-related formin family involved in cytoskeletal rearrangements and a downstream effector of  
318 RhoA. Consistent with these reports, other groups have shown that many viruses including adenoviruses and the  
319 *alphaherpesvirus*, HSV-1, travel along stabilized microtubules. Sodeik et al. showed that stabilization of  
320 microtubules with paclitaxel prior to HSV-1 infection had no effect on the nuclear accumulation of capsids  
321 (Sodeik et al., 1997) and Mabit et al. showed that paclitaxel treatment slightly increased nuclear delivery of  
322 capsids (Mabit et al., 2002). These studies revealed that microtubule dynamics, or treadmilling, are not required  
323 for HSV-1 capsid trafficking. The finding in our current study that EHV-1 infection actively induces the  
324 stabilization of microtubules and that infection is not negatively affected by the prior stabilization of  
325 microtubules suggests a common mechanism of microtubule transport of nucleocapsids that is shared amongst  
326 alphaherpesviruses.

327 The connection between EHV-1-induced microtubule stabilization, virus trafficking along stabilized  
328 microtubules, and the dependence of virus trafficking on ROCK1 function would suggest a direct role for the  
329 RhoA-ROCK1 signaling pathway in microtubule stabilization. However, one group showed that while RhoA is  
330 required for this effect, it is not mediated through ROCK1 (Palazzo et al., 2001). Consistent with these data, our  
331 results revealed that the inhibition of EHV-1 infection by Y-27632 did not inhibit EHV-1-induced stabilization  
332 of microtubules. We therefore concluded that the contribution of ROCK1 to virus trafficking is most likely  
333 separate from virus-induced microtubule stabilization.

334 The observation that many virus particles remain associated with the plasma membrane in the presence of  
335 the ROCK1 inhibitor Y-27632 suggests other possible roles for ROCK1 in virus trafficking. Two intriguing  
336 possibilities are that 1) ROCK1 activity is required in order to mediate an interaction between virus and  
337 microtubules and/or other cytoskeletal components or 2) ROCK1 is required for efficient fusion of the viral  
338 envelope with a cellular membrane. Inhibition of either of these processes could account for the inability of  
339 EHV-1 to traffic to the nucleus. Future studies will examine which virus components are involved in the

340 initiation of signaling pathways that lead to both ROCK1 activation and separately the acetylation of  
341 microtubules.

## 343 5. Conclusion

344 In the current study we examined some of the early interactions between EHV-1 and host cell factors and, in  
345 particular, investigated how EHV-1 utilizes the cell's microtubular network and associated proteins to  
346 efficiently infect susceptible cells. Our results showed that disruption of microtubules by the addition of  
347 microtubule-depolymerizing agents and the inhibition of the microtubule motor protein, dynein, significantly  
348 abrogated EHV-1 infection in ED and CHO-K1 cells. Our data also revealed that stabilization of microtubules  
349 by paclitaxel prior to infection had no impact on the efficiency of EHV-1 infection in either cell type.  
350 Interestingly, our data showed that microtubules are acetylated very early after infection with EHV-1. Whether  
351 this acetylation is an absolute requirement for EHV-1 infection is an intriguing question and efforts are  
352 underway to address this possibility. Finally, we showed that inhibition of the cellular kinase ROCK1 with the  
353 drug Y-27632, inhibited the movement of EHV-1 capsids to the nucleus. These ROCK1 data follow-up on our  
354 earlier study, showing that ROCK1 activation is critical for EHV-1 infection (Frampton et al., 2007). Future  
355 studies will aim to define how ROCK1 is activated by EHV-1, what specific cellular events are reliant upon this  
356 activation, and how these cellular events contribute to a productive infection. Knowledge obtained from these  
357 studies may be translated into the development of antiviral compounds that can be used to inhibit the identified  
358 critical processes that EHV-1 needs to complete its pathogenic program within the horse.

## 360 Acknowledgments

361 We thank Patricia Spear for providing the CHO cell lines and Ron Montelaro for the ED cells. We thank Simon  
362 Watkins for the use of the confocal microscope. This work was supported by NIH grants CA119298, NS44323,  
363 NS040923, and HL066949.

## 366 References

- 367 ALLEN, G. P., AND J.T. BRYANS (1986) Molecular epizootiology, pathogenesis, and prophylaxis of equine  
 368 herpesvirus-1 infections. *Prog. Vet. Microbiol. Immunol.*, 2, 78-144.
- 369 ALONSO, C., MISKIN, J., HERNAEZ, B., FERNANDEZ-ZAPATERO, P., SOTO, L., CANTO, C.,  
 370 RODRIGUEZ-CRESPO, I., DIXON, L. & ESCRIBANO, J. M. (2001) African swine fever virus protein  
 371 p54 interacts with the microtubular motor complex through direct binding to light-chain dynein. *J Virol*,  
 372 75, 9819-27.
- 373 BOUCHARD, P., PENNINGROTH, S. M., CHEUNG, A., GAGNON, C. & BARDIN, C. W. (1981) erythro-9-  
 374 [3-(2-Hydroxynonyl)]adenine is an inhibitor of sperm motility that blocks dynein ATPase and protein  
 375 carboxylmethylase activities. *Proc Natl Acad Sci U S A*, 78, 1033-6.
- 376 CHESHENKO, N., LIU, W., SATLIN, L. M. & HEROLD, B. C. (2005) Focal adhesion kinase plays a pivotal  
 377 role in herpes simplex virus entry. *J Biol Chem*, 280, 31116-25.
- 378 CHEUNG, P. Y., ZHANG, Y., LONG, J., LIN, S., ZHANG, M., JIANG, Y. & WU, Z. (2004) p150(Glued),  
 379 Dynein, and microtubules are specifically required for activation of MKK3/6 and p38 MAPKs. *J Biol*  
 380 *Chem*, 279, 45308-11.
- 381 CLEMENT, C., TIWARI, V., SCANLAN, P. M., VALYI-NAGY, T., YUE, B. Y. & SHUKLA, D. (2006) A  
 382 novel role for phagocytosis-like uptake in herpes simplex virus entry. *J Cell Biol*, 174, 1009-21.
- 383 CSELLNER, H., WALKER, C., WELLINGTON, J. E., MCLURE, L. E., LOVE, D. N. & WHALLEY, J. M.  
 384 (2000) EHV-1 glycoprotein D (EHV-1 gD) is required for virus entry and cell-cell fusion, and an EHV-  
 385 1 gD deletion mutant induces a protective immune response in mice. *Arch Virol*, 145, 2371-85.
- 386 DHANI, S. U., MOHAMMAD-PANAH, R., AHMED, N., ACKERLEY, C., RAMJEESINGH, M. & BEAR,  
 387 C. E. (2003) Evidence for a functional interaction between the CIC-2 chloride channel and the  
 388 retrograde motor dynein complex. *J Biol Chem*, 278, 16262-70.
- 389 DOHNER, K., NAGEL, C. H. & SODEIK, B. (2005) Viral stop-and-go along microtubules: taking a ride with  
 390 dynein and kinesins. *Trends Microbiol*, 13, 320-7.
- 391 DOHNER, K., WOLFSTEIN, A., PRANK, U., ECHEVERRI, C., DUJARDIN, D., VALLEE, R. & SODEIK,  
 392 B. (2002) Function of dynein and dynactin in herpes simplex virus capsid transport. *Mol Biol Cell*, 13,  
 393 2795-809.
- 394 DOUGLAS, M. W., DIEFENBACH, R. J., HOMA, F. L., MIRANDA-SAKSENA, M., RIXON, F. J.,  
 395 VITTONI, V., BYTH, K. & CUNNINGHAM, A. L. (2004) Herpes simplex virus type 1 capsid protein  
 396 VP26 interacts with dynein light chains RP3 and Tctex1 and plays a role in retrograde cellular transport.  
 397 *J Biol Chem*, 279, 28522-30.
- 398 ELLIOTT, G. & O'HARE, P. (1998) Herpes simplex virus type 1 tegument protein VP22 induces the  
 399 stabilization and hyperacetylation of microtubules. *J Virol*, 72, 6448-55.
- 400 FLORIN, L., BECKER, K. A., LAMBERT, C., NOWAK, T., SAPP, C., STRAND, D., STREECK, R. E. &  
 401 SAPP, M. (2006) Identification of a dynein interacting domain in the papillomavirus minor capsid  
 402 protein 12. *J Virol*, 80, 6691-6.
- 403 FRAMPTON, A. R., JR., GOINS, W. F., COHEN, J. B., VON EINEM, J., OSTERRIEDER, N.,  
 404 O'CALLAGHAN, D. J. & GLORIOSO, J. C. (2005) Equine herpesvirus 1 utilizes a novel herpesvirus  
 405 entry receptor. *J Virol*, 79, 3169-73.
- 406 FRAMPTON, A. R., JR., SMITH, P. M., ZHANG, Y., MATSUMURA, T., OSTERRIEDER, N. &  
 407 O'CALLAGHAN, D. J. (2002) Contribution of gene products encoded within the unique short segment  
 408 of equine herpesvirus 1 to virulence in a murine model. *Virus Res*, 90, 287-301.
- 409 FRAMPTON, A. R., JR., STOLZ, D. B., UCHIDA, H., GOINS, W. F., COHEN, J. B. & GLORIOSO, J. C.  
 410 (2007) Equine Herpesvirus 1 Enters Cells by Two Different Pathways, and Infection Requires the  
 411 Activation of the Cellular Kinase ROCK1. *J Virol*, 81, 10879-89.
- 412 JACOB, Y., BADRANE, H., CECCALDI, P. E. & TORDO, N. (2000) Cytoplasmic dynein LC8 interacts with  
 413 lyssavirus phosphoprotein. *J Virol*, 74, 10217-22.

- 414 JOUVENET, N., MONAGHAN, P., WAY, M. & WILEMAN, T. (2004) Transport of African swine fever virus  
 415 from assembly sites to the plasma membrane is dependent on microtubules and conventional kinesin. *J*  
 416 *Virol*, 78, 7990-8001.
- 417 KELKAR, S. A., PFISTER, K. K., CRYSTAL, R. G. & LEOPOLD, P. L. (2004) Cytoplasmic dynein mediates  
 418 adenovirus binding to microtubules. *J Virol*, 78, 10122-32.
- 419 KOBAYASHI, T., MARTENSEN, T., NATH, J. & FLAVIN, M. (1978) Inhibition of dynein ATPase by  
 420 vanadate, and its possible use as a probe for the role of dynein in cytoplasmic motility. *Biochem Biophys*  
 421 *Res Commun*, 81, 1313-8.
- 422 KRISTENSSON, K., LYCKE, E., ROYTTA, M., SVENNERHOLM, B. & VAHLNE, A. (1986) Neuritic  
 423 transport of herpes simplex virus in rat sensory neurons in vitro. Effects of substances interacting with  
 424 microtubular function and axonal flow [nocodazole, taxol and erythro-9-3-(2-hydroxynonyl)adenine]. *J*  
 425 *Gen Virol*, 67 ( Pt 9), 2023-8.
- 426 LEE, G. E., MURRAY, J. W., WOLKOFF, A. W. & WILSON, D. W. (2006) Reconstitution of herpes simplex  
 427 virus microtubule-dependent trafficking in vitro. *J Virol*, 80, 4264-75.
- 428 MABIT, H., NAKANO, M. Y., PRANK, U., SAAM, B., DOHNER, K., SODEIK, B. & GREBER, U. F. (2002)  
 429 Intact microtubules support adenovirus and herpes simplex virus infections. *J Virol*, 76, 9962-71.
- 430 NARANATT, P. P., KRISHNAN, H. H., SMITH, M. S. & CHANDRAN, B. (2005) Kaposi's sarcoma-  
 431 associated herpesvirus modulates microtubule dynamics via RhoA-GTP-diphosphoinositol 2 signaling and  
 432 utilizes the dynein motors to deliver its DNA to the nucleus. *J Virol*, 79, 1191-206.
- 433 NOGALES, E. (2000) Structural insights into microtubule function. *Annu Rev Biochem*, 69, 277-302.
- 434 O'CALLAGHAN, D. J., GENTRY, G. A. & RANDALL, C. C. (1983) The equine herpesviruses. IN  
 435 ROIZMAN, B. (Ed.) *The Herpesviruses, Comprehensive Virology*. New York, Plenum Press.
- 436 OSTERRIEDER, N. (1999) Construction and characterization of an equine herpesvirus 1 glycoprotein C  
 437 negative mutant. *Virus Res*, 59, 165-77.
- 438 PALAZZO, A. F., COOK, T. A., ALBERTS, A. S. & GUNDERSEN, G. G. (2001) mDia mediates Rho-  
 439 regulated formation and orientation of stable microtubules. *Nat Cell Biol*, 3, 723-9.
- 440 PENNINGROTH, S. M., CHEUNG, A., BOUCHARD, P., GAGNON, C. & BARDIN, C. W. (1982) Dynein  
 441 ATPase is inhibited selectively in vitro by erythro-9-[3-2-(hydroxynonyl)]adenine. *Biochem Biophys*  
 442 *Res Commun*, 104, 234-40.
- 443 PETIT, C., GIRON, M. L., TOBALY-TAPIERO, J., BITTOUN, P., REAL, E., JACOB, Y., TORDO, N., DE  
 444 THE, H. & SAIB, A. (2003) Targeting of incoming retroviral Gag to the centrosome involves a direct  
 445 interaction with the dynein light chain 8. *J Cell Sci*, 116, 3433-42.
- 446 PIPERNO, G., LEDIZET, M. & CHANG, X. J. (1987) Microtubules containing acetylated alpha-tubulin in  
 447 mammalian cells in culture. *J Cell Biol*, 104, 289-302.
- 448 RAGHU, H., SHARMA-WALIA, N., VEETIL, M. V., SADAGOPAN, S., CABALLERO, A.,  
 449 SIVAKUMAR, R., VARGA, L., BOTTERO, V. & CHANDRAN, B. (2007) Lipid rafts of primary  
 450 endothelial cells are essential for Kaposi's sarcoma-associated herpesvirus/human herpesvirus 8-induced  
 451 phosphatidylinositol 3-kinase and RhoA-GTPases critical for microtubule dynamics and nuclear  
 452 delivery of viral DNA but dispensable for binding and entry. *J Virol*, 81, 7941-59.
- 453 RAUX, H., FLAMAND, A. & BLONDEL, D. (2000) Interaction of the rabies virus P protein with the LC8  
 454 dynein light chain. *J Virol*, 74, 10212-6.
- 455 RAVIKUMAR, B., ACEVEDO-AROZENA, A., IMARISIO, S., BERGER, Z., VACHER, C., O'KANE, C. J.,  
 456 BROWN, S. D. & RUBINSZTEIN, D. C. (2005) Dynein mutations impair autophagic clearance of  
 457 aggregate-prone proteins. *Nat Genet*, 37, 771-6.
- 458 SODEIK, B., EBERSOLD, M. W. & HELENIUS, A. (1997) Microtubule-mediated transport of incoming  
 459 herpes simplex virus 1 capsids to the nucleus. *J Cell Biol*, 136, 1007-21.
- 460 SUGAHARA, Y., MATSUMURA, T., KONO, Y., HONDA, E., KIDA, H. & OKAZAKI, K. (1997)  
 461 Adaptation of equine herpesvirus 1 to unnatural host led to mutation of the gC resulting in increased  
 462 susceptibility of the virus to heparin. *Arch Virol*, 142, 1849-56.

463 SUIKKANEN, S., AALTONEN, T., NEVALAINEN, M., VALILEHTO, O., LINDHOLM, L., VUENTO, M.  
464 & VIHINEN-RANTA, M. (2003) Exploitation of microtubule cytoskeleton and dynein during  
465 parvoviral traffic toward the nucleus. *J Virol*, 77, 10270-9.

466 YE, G. J., VAUGHAN, K. T., VALLEE, R. B. & ROIZMAN, B. (2000) The herpes simplex virus 1 U(L)34  
467 protein interacts with a cytoplasmic dynein intermediate chain and targets nuclear membrane. *J Virol*,  
468 74, 1355-63.

469  
470  
471  
472  
473  
474  
475  
476  
477  
478  
479  
480  
481  
482  
483  
484  
485  
486  
487  
488  
489  
490  
491  
492  
493  
494  
495  
496  
497  
498  
499

500

501

502

503

504

505

506

**Figure Legends**

**Fig. 1.** Depolymerization of microtubules inhibits EHV-1 infection. Triplicate cultures of ED cells were mock-treated or treated with increasing amounts of the microtubule depolymerizing drugs (A) nocodazole, (B) vinblastine, or (C) colchicine for 30 min at 37°C and then infected with EHV-1 (L11ΔgIΔgE) at an MOI of 5 for 5.5 h in the presence of the drugs. β-galactosidase expression was measured by an ONPG assay (filled circles). Absorbance at 405nm was measured for each sample and  $A_{405nm}$  values from infected cells that were not treated with drug were set as 100% infection. Cell viability at each concentration of drug was measured by an MTS assay (open circles) and viability of cells that were not treated with drug was set at 100%.

**Fig. 2.** Stabilization of microtubules does not inhibit EHV-1 infection. Triplicate cultures of ED (A) or CHO-K1 (B) cells were mock-treated or treated with increasing amounts of the microtubule-stabilizing compound, paclitaxel (PTX) for 30 min at 37°C and then infected with EHV-1 (L11ΔgIΔgE) at an MOI of 5 for 5.5 h in the presence of the drug. β-galactosidase expression was measured by an ONPG assay (filled circles). Absorbance at 405nm was measured for each sample and  $A_{405nm}$  values from infected cells that were not treated with drug were set as 100% infection.

**Fig. 3.** Paclitaxel (PTX) stabilization of microtubules. ED cells were serum-starved for 1 h and then mock-treated or treated with 10 μM of paclitaxel for 15, 30, or 60 min. Acetylated and total tubulin were detected by western blot as described in Materials and Methods.

**Fig. 4.** Paclitaxel (PTX) treatment of cells has no effect on EHV-1 infection. CHO-K1 cells were mock treated or treated with 10 μM of PTX for 30 min at 37°C. Cells were chilled on ice for 10 min and then L11VP26mRed was incubated on the cells at 4°C for 2 h in the presence or absence of PTX (10μM). 37°C media with or without PTX was added to the cells and then the cells were fixed and stained at 0 and 60 min with Hoechst and wheat germ agglutinin to label the nucleus (blue) and plasma membrane (green), respectively. Capsids (red) were observed with a confocal microscope. White arrows indicate peri-nuclear capsids.

533

534 **Fig. 5.** EHV-1 induces the acetylation of tubulin. ED cells were serum starved for 1 h and then mock-treated or  
535 treated with Y-27632 for 30 min. Cells were mock-infected or infected with EHV-1 (L11VP26mRed) at an  
536 MOI of 10 in the presence or absence of Y-27632. Acetylated and total tubulin were detected by western blot at  
537 15, 30, and 60 min post-infection as described in Materials and Methods.

538

539 **Fig. 6.** Inhibition of dynein with EHNA blocks EHV-1 infection. Triplicate cultures of (A) ED or (B) CHO-K1  
540 cells were mock-treated or treated with increasing amounts of EHNA (filled circles) or AMP-PNP (filled  
541 diamonds) for 30 min at 37°C and then infected with EHV-1 (L11ΔgIΔgE) at an MOI of 5 for 5.5 h in the  
542 presence of the drugs. β-galactosidase expression was measured by ONPG assay and cell viability at each  
543 concentration of drug was measured by MTS assay, EHNA (open circles), AMP-PNP (open diamonds).

544

545 **Fig. 7.** Increased infectious EHV-1 recovery in the presence of the ROCK inhibitor, Y-27632. Triplicate  
546 cultures of CHO-K1 cells were either mock-treated (open circles) or treated with 100 μM of Y-27632 (closed  
547 circles) for 30 min at 37°C. Cells were chilled on ice for 10 min and then L11ΔgIΔgE at an MOI of 10 was  
548 bound to the cells at 4°C for 2h in the presence or absence of Y-27632. Cells were washed and cold media was  
549 replaced with 37°C media. At the indicated times, cells were treated with an acidic buffer (pH 3.0) to inactivate  
550 non-internalized virus and the cells were washed with media. Internalized virus was harvested from cells and  
551 titered on RK13 cells.

552

553 **Fig. 8.** (A) CHO-K1 cells were mock treated (top panels) or (B) treated with 100 μM Y-27632 for 30 min at  
554 37°C. Cells were chilled on ice for 10 min and then L11VP26mRed (MOI 10) was incubated on the cells at 4°C  
555 for 2 h in the absence (A) or presence (B) of Y-27632 (100 μM). 37°C media with or without Y-27632 was  
556 added to the cells and then the cells were fixed and stained at 0, 15, 30, 60, and 120 min. with Hoechst and  
557 wheat germ agglutinin to label the nucleus (blue) and plasma membrane (green), respectively. Capsids (red)

558 were observed with a confocal microscope. Nuclear-associated capsids are circled in white and non-nuclear  
559 associated capsids are circled in yellow.

Accepted Manuscript

Fig. 1A.

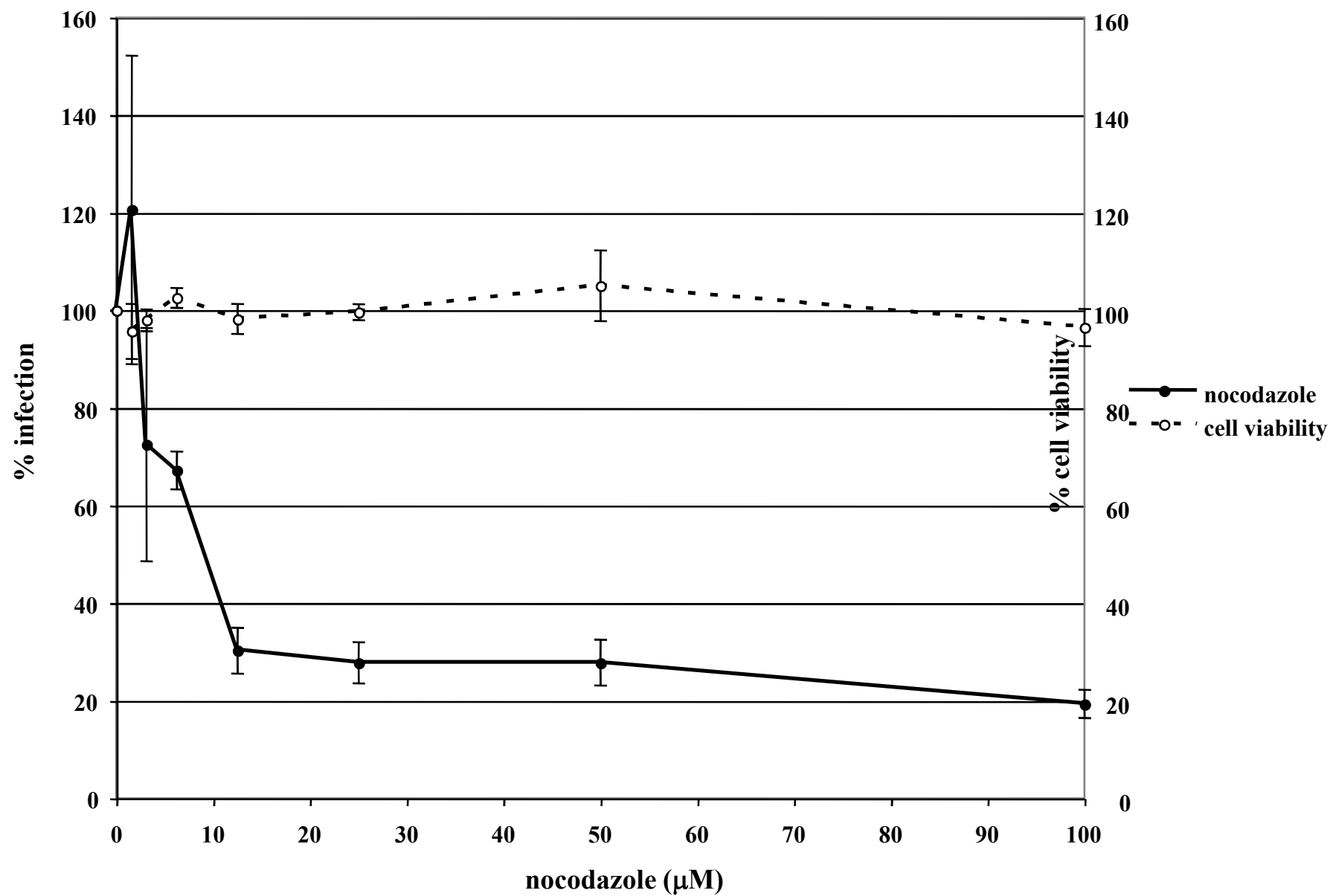


Fig. 1B.

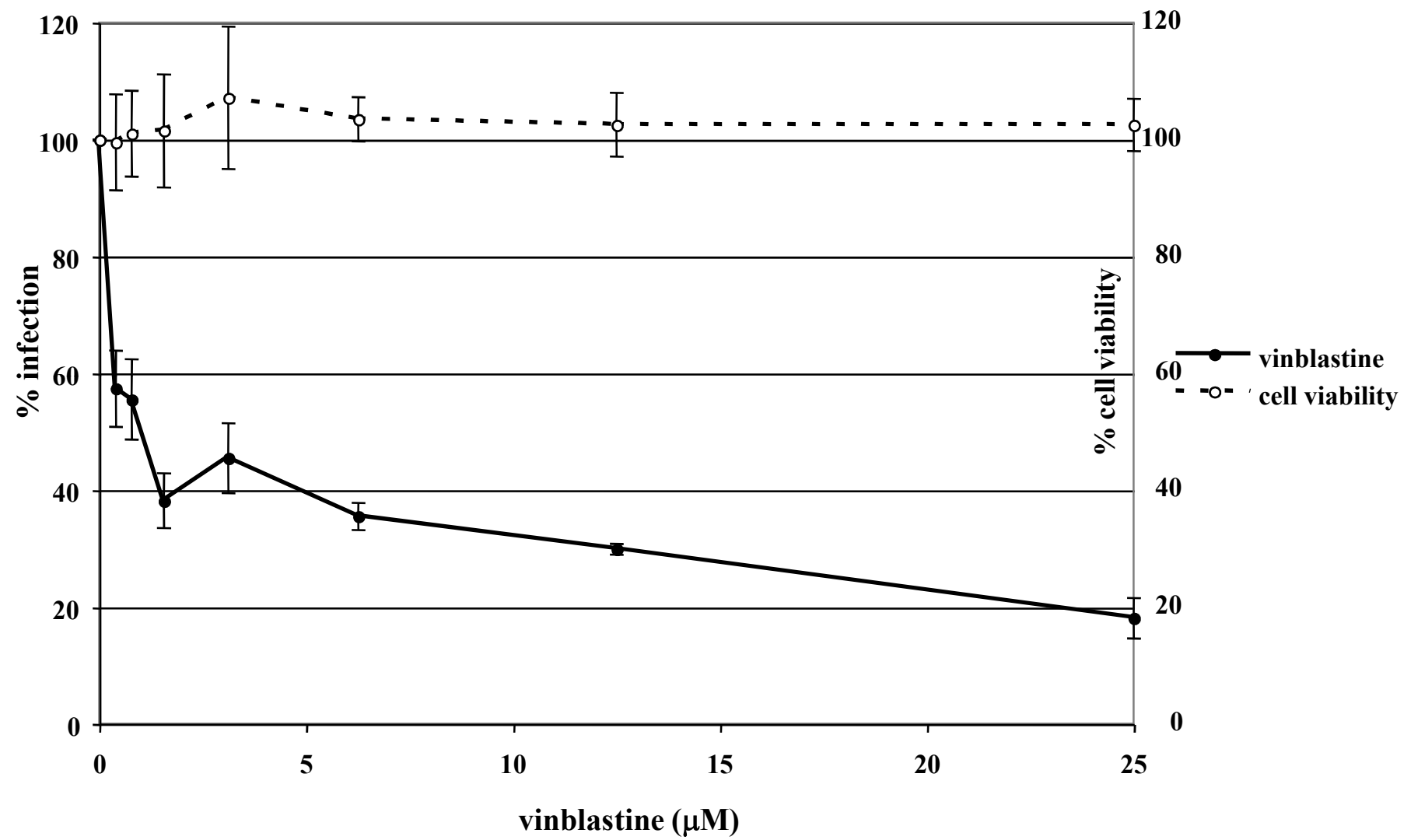


Fig. 1C.

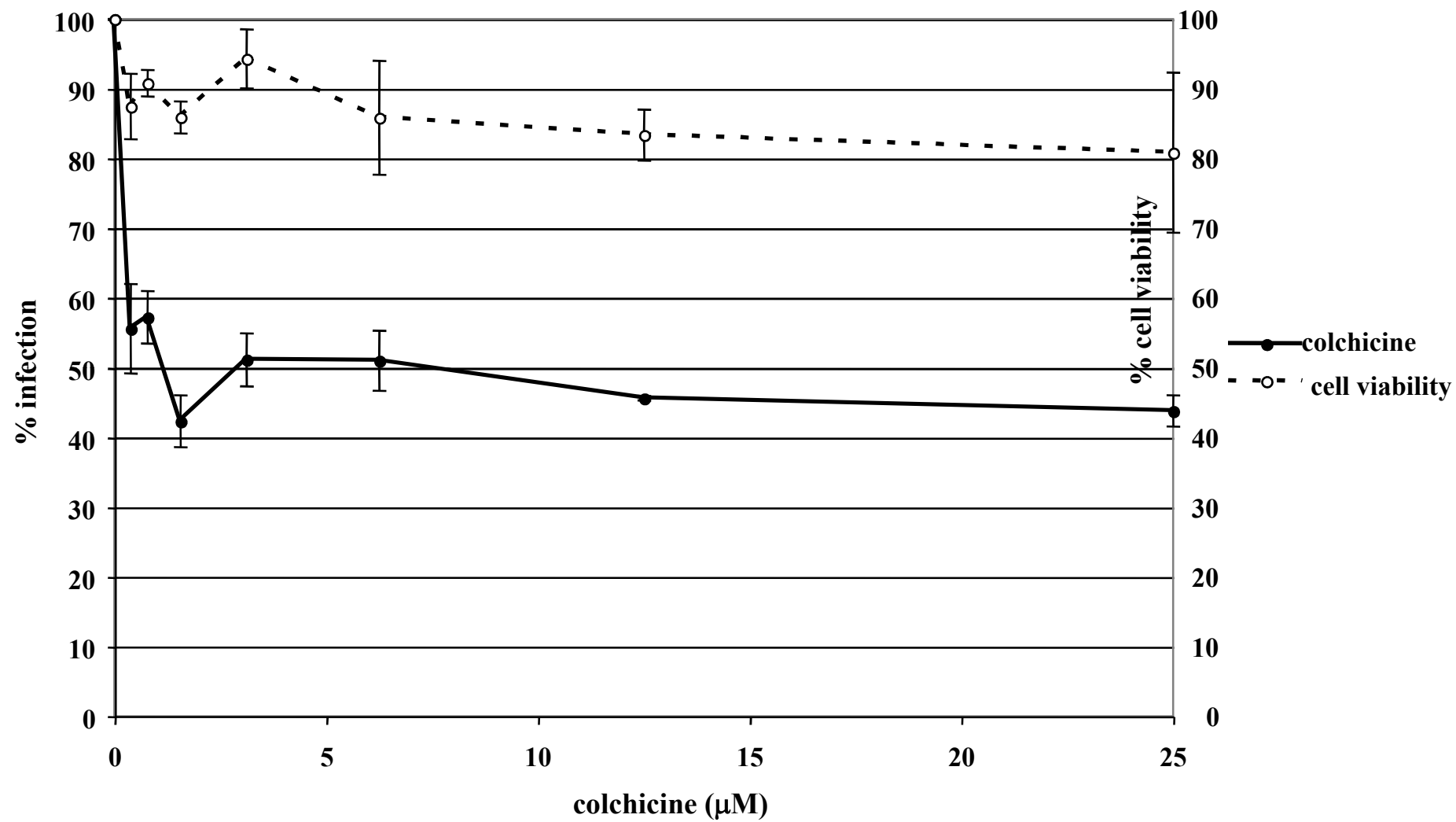


Fig. 2A.

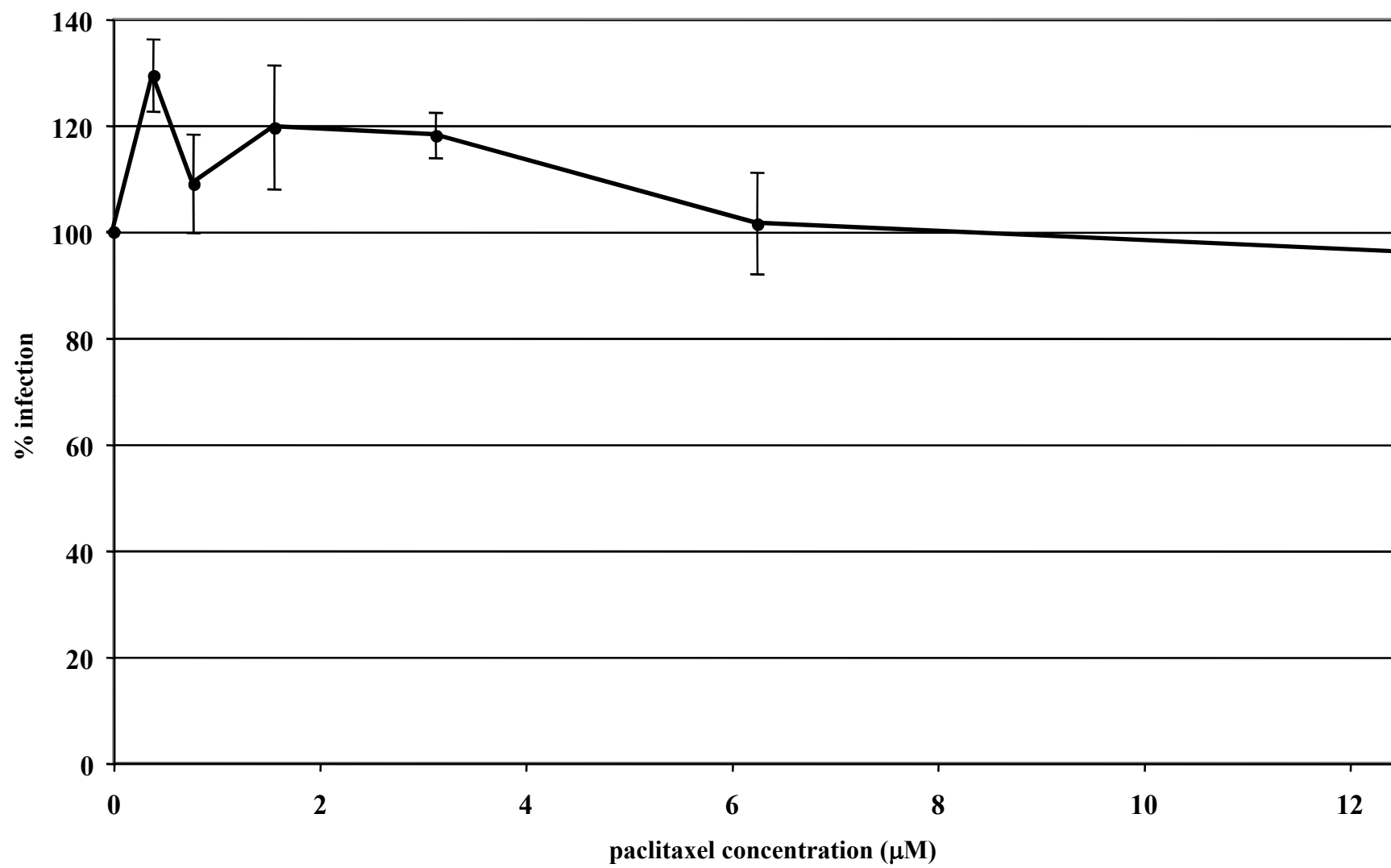


Fig. 2B.

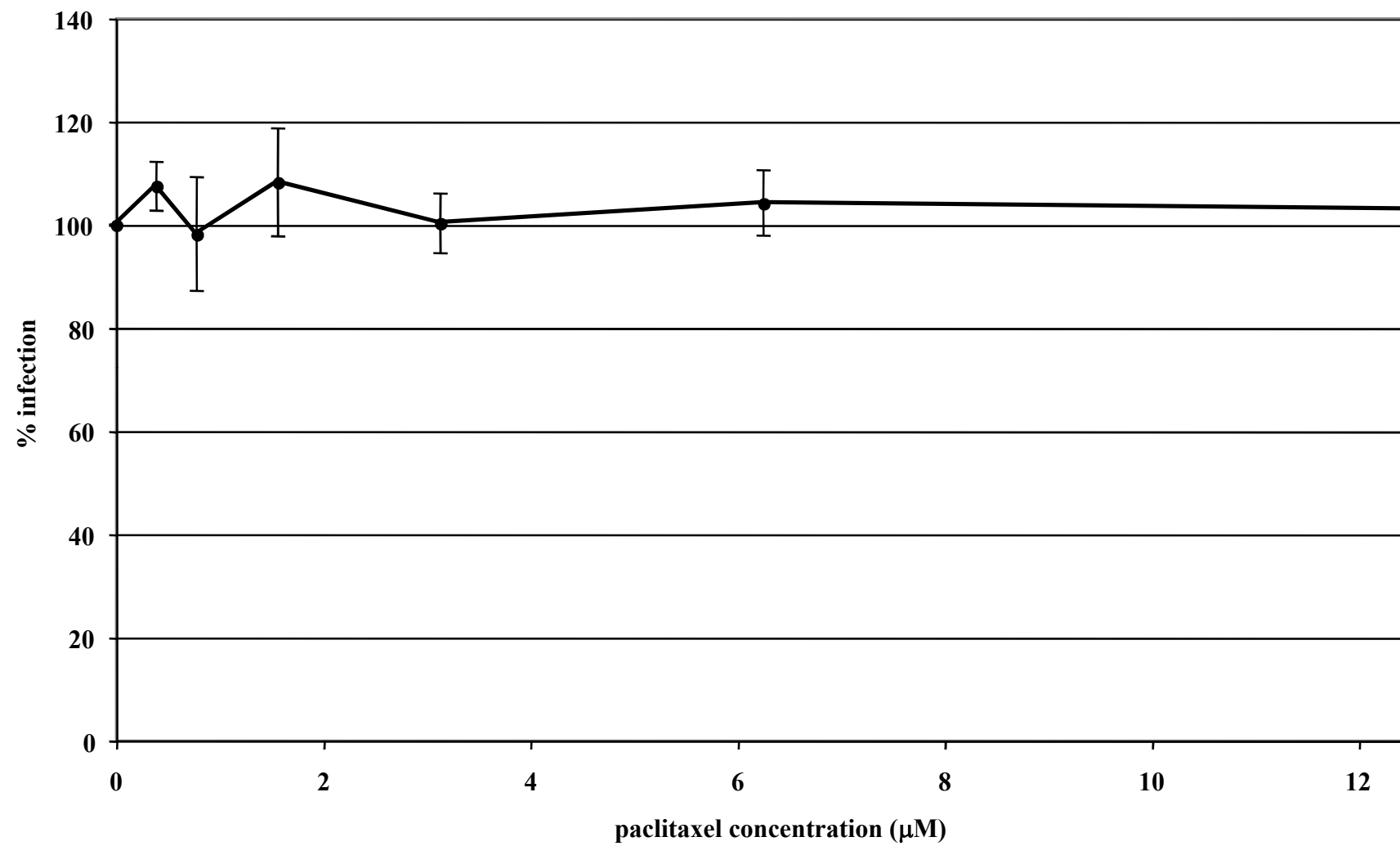
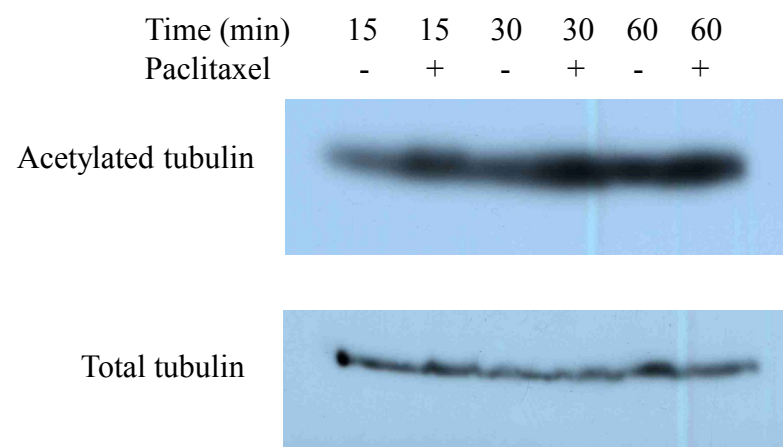


Fig. 3.



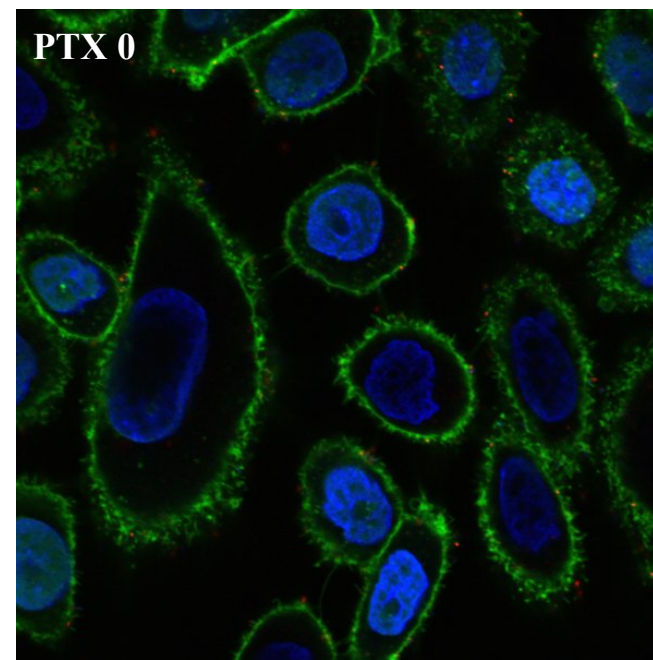
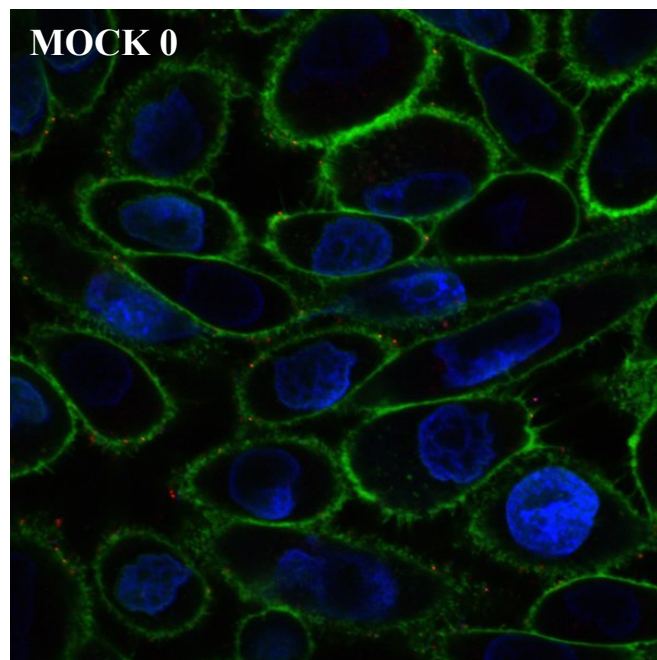


Fig. 4.

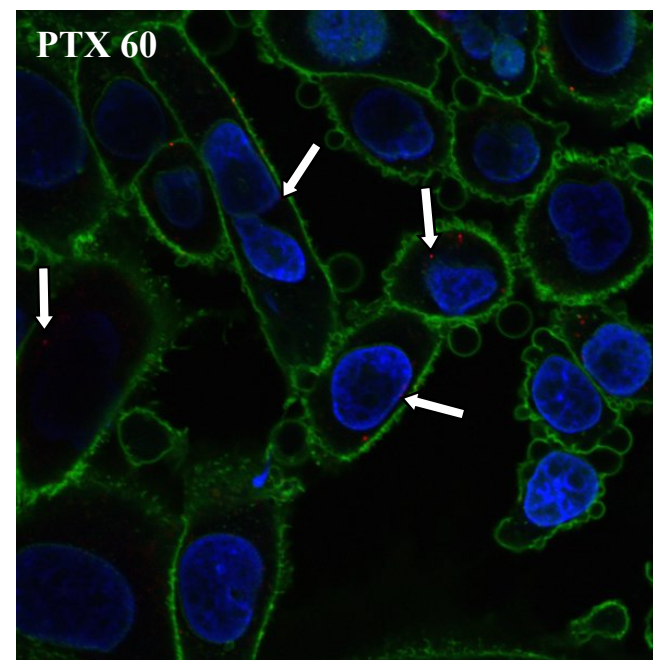
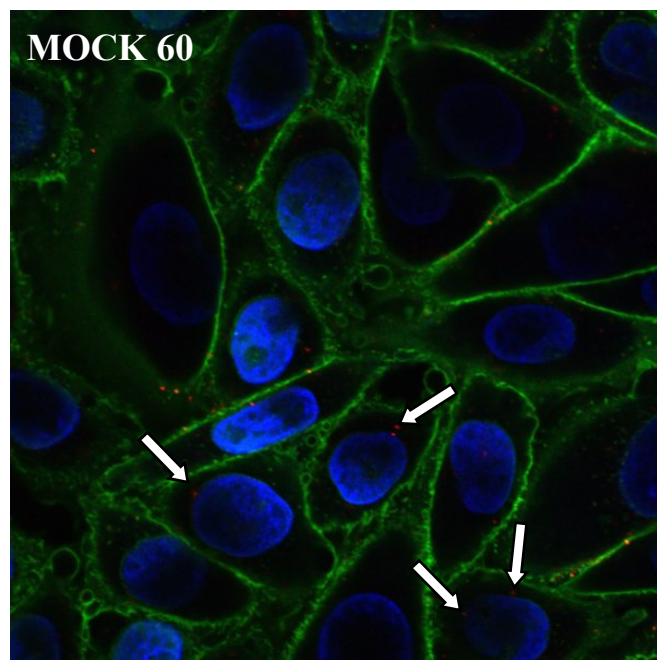


Fig. 5.

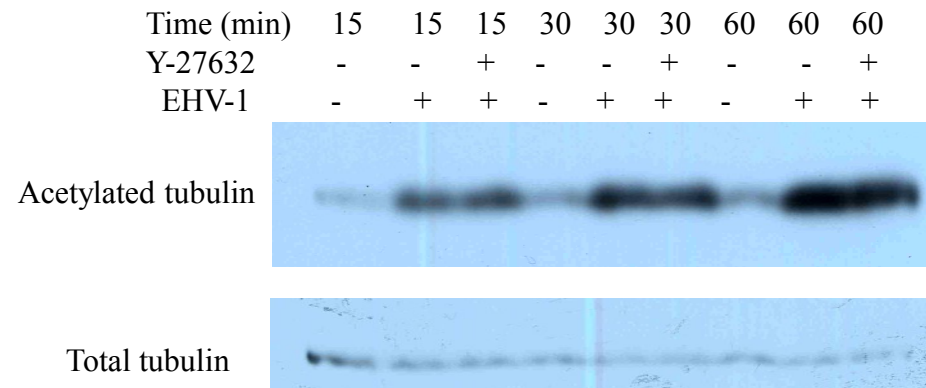


Fig. 6A.

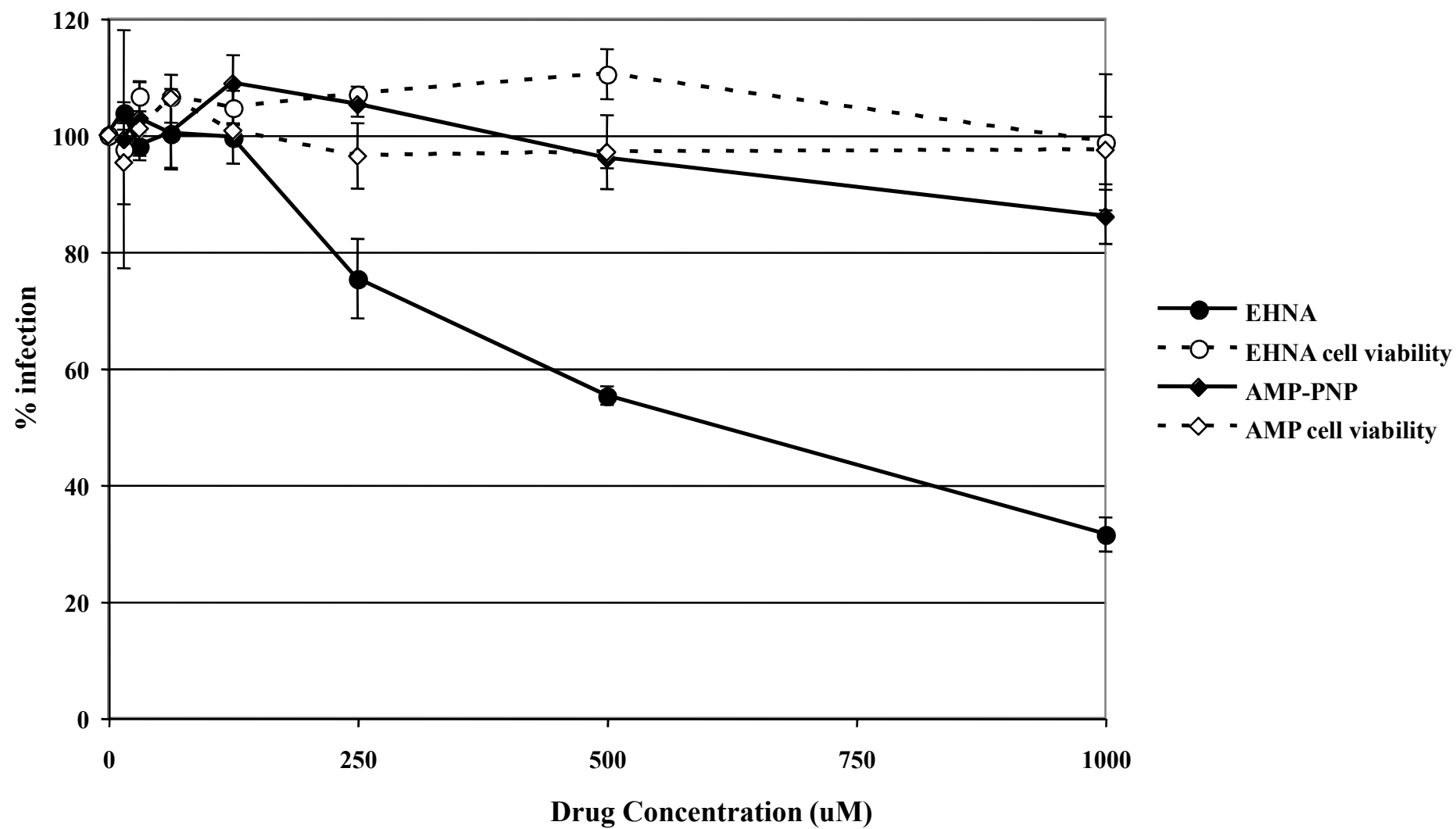


Fig. 6B.

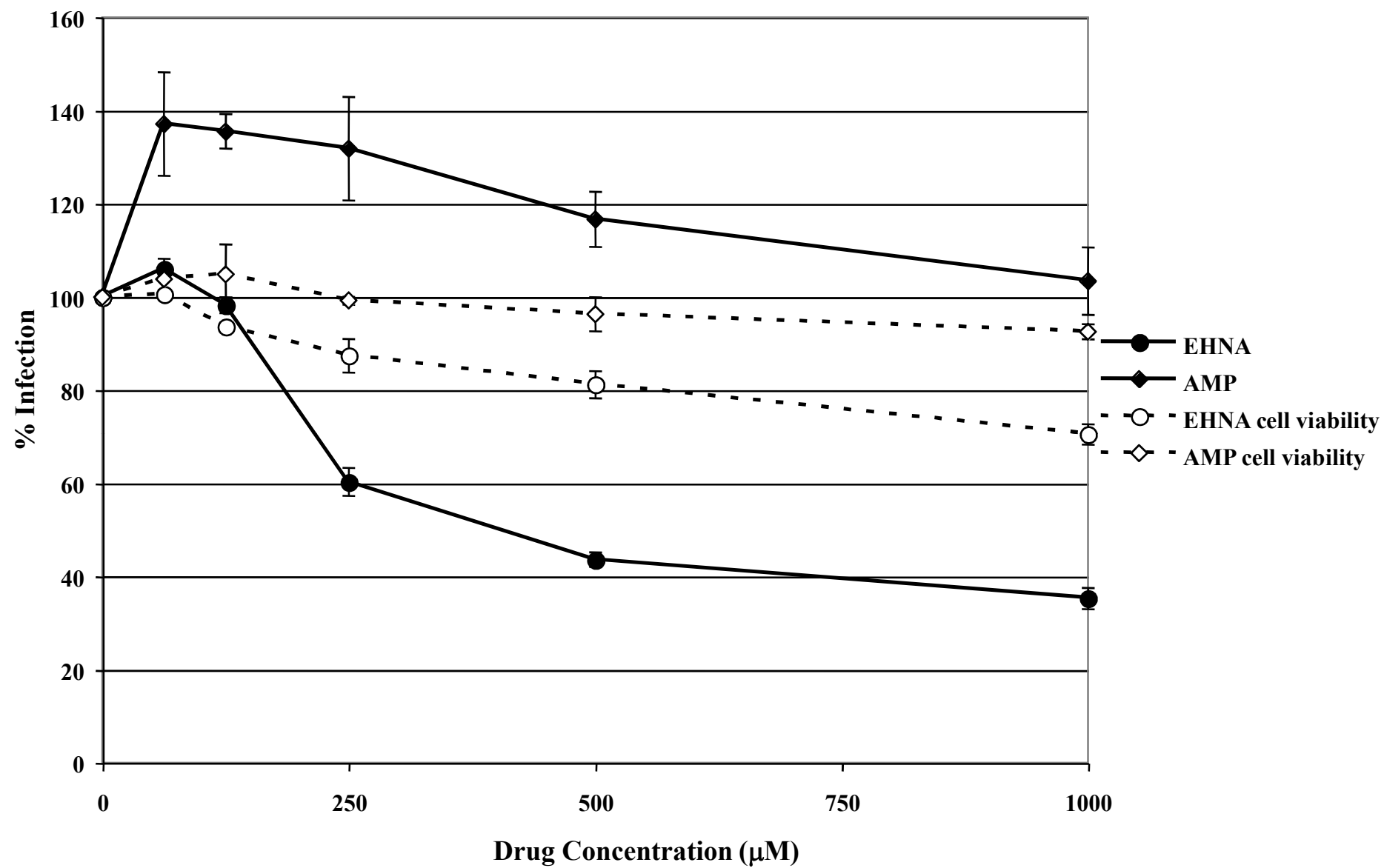


Fig. 7.

